NASA TN D-166

TECHNICAL NOTE

D-166

A HYDRODYNAMIC INVESTIGATION OF THE EFFECT OF ADDING UPPER-SURFACE CAMBER TO A SUBMERGED FLAT PLATE

By Victor L. Vaughan, Jr.

Langley Research Center
Langley Field, Va.

NATIONAL AERONAUTICS AND SPACE ADMINISTRATION

WASHINGTON November 1959

NATIONAL AERONAUTICS AND SPACE ADMINISTRATION

TECHNICAL NOTE D-166

A HYDRODYNAMIC INVESTIGATION OF THE EFFECT OF ADDING UPPER-SURFACE CAMBER TO A SUBMERGED FLAT PLATE

By Victor L. Vaughan, Jr.

SUMMARY

A hydrodynamic investigation has been conducted to determine the effects of adding camber to the upper surface of a rectangular modified flat plate having an aspect ratio of 0.25 and operating at a constant depth of submersion of 6 inches at noncavitating and nonventilating speeds. Comparisons have been made between these data and data previously obtained on two rectangular modified flat plates having aspect ratios of 0.25 with different thicknesses. These comparisons show that adding camber to the upper surface of a flat plate, which increased the thickness, decreased the angle of zero lift, the lift-curve slope, and the lift coefficients at the high angles of attack. The addition of camber moved the center-of-pressure location rearward with decreasing angle of attack while the center-of-pressure location of the flat plates moved forward with decreasing angle of attack. For a given lift coefficient the lift-drag ratio decreased with increasing camber. The maximum lift-drag ratio moved to higher angles of attack with increasing camber. As the camber on the upper surface was increased, thus increasing the thickness from approximately 7- to 10-percent chord, the lift coefficient increased as a linear function of thickness.

INTRODUCTION

As part of a program to determine the hydrodynamic characteristics of submerged low-aspect-ratio lifting surfaces, the Langley Research Center has been conducting investigations on rectangular modified flat plates. The results of these investigations are reported in references 1 to 4. The present investigation was undertaken to obtain information on the effects of increasing the thickness by adding upper-surface camber. The investigation was conducted in Langley tank no. 2 on three models having different upper-surface airfoil sections: an NACA 64_1A412 section, an NACA 64_1A212 section, and a modified NACA 64_1A412 section. The tests were made at a constant depth of submersion at noncavitating and nonventilating speeds. This paper presents the results of the investigation

and shows comparisons with data previously obtained on two flat-plate models having different thicknesses (refs. 1 and 2).

APPARATUS AND PROCEDURE

Description of Models

The three models were rectangular in plan form, had aspect ratios of 0.25, and were mounted on a single strut as shown in figure 1. They had the same plan-form shape and area (50 sq in.) as the aspect-ratio-0.25 rectangular modified flat plates reported in references 1 to 4. The lower surfaces were flat with the leading edges rounded to 2:1 ellipses and with the trailing edges beveled so that they formed 5° angles with the chord lines of the models. These lower surfaces were the same as the lower surface of the aspect-ratio-0.25 flat plate described in reference 1. The upper surfaces were cambered and each model had a different thickness as a result of the different amounts of camber. The coordinates for the upper surfaces are presented in tables I, II, and III. An NACA 64_1A412 airfoil section was used for the upper surface of the thick cambered model and an NACA 64_1A212 airfoil section was used for the upper surface of the medium cambered model. The thin cambered model had a modified NACA 64_1A412 airfoil section for the upper surface. The thicknesses of the models were 9.88, 8.60, and 7.02 percent chord, respectively. The models were made with a steel inner core covered with plastic which was polished to a smooth finish. A photograph of a typical model is presented in figure 2.

The strut used (also shown in figs. 1 and 2) had an NACA 66_1-012 airfoil section and was the same strut that was used in the investigation reported in reference 1. The strut was mounted so that the leading edge was 8.19 inches forward of the trailing edge of the model and was perpendicular to the chord line of the model. There were no fillets at the intersection of the strut and model. The strut was made of stainless steel and polished to a smooth finish.

Test Methods and Equipment

Tests were made by using the Langley tank no. 2 towing carriage with electrical strain-gage balances to measure independently the lift, drag, and pitching moment. The pitching moment was measured about an arbitrary point above the model, and the data obtained were used to calculate the pitching moment about the trailing edge of the model.

For all tests a wind screen was used to reduce the aerodynamic tares and aerodynamic effects on the flow pattern to negligible values. Force measurements were made at constant speeds for fixed angles of attack and depth of submersion. Depth of submersion is defined as the distance from the undisturbed water surface to the chord line of the model at the leading edge. The chord line is defined as the line which is parallel to the lower surface and which passes through the trailing edge (fig. 1). Tests were made at a depth of submersion of 6 inches over a range of angles of attack from 0° to 20° and at speeds up to 30 fps.

L
3
1
9

The changes in angle of attack and the accompanying changes in depth of submersion due to the structural deflections were measured during the calibration of the balances and found to be negligible for the combination of forces encountered. The estimated accuracy of the measurements is as follows:

Angle of attack, deg	±0.1
Depth of submersion, in.	±0.1
Speed, fps	±0.2
Lift, lb	±3.0
Drag, lb	±1.0
Pitching moment, ft-lb	±0.3

The forces and moments were converted to the usual aerodynamic-coefficient form by using a measured value of the density of water of 1.942 slugs/cu ft. The kinematic viscosity measured during the tests was 1.67×10^{-5} ft^2/sec.

DISCUSSION AND RESULTS

General Force Data

The basic experimental data are presented in figures 3 to 5 as plots of lift, drag, and pitching moment about the trailing edge as a function of speed with angle of attack as the parameter. Data are given for each of the three models tested.

Effects of Upper-Surface Camber

The lift characteristics of the upper-surface-camber models and of the rectangular modified flat-plate models (refs. 1 and 2) are compared in figure 6. Each model is identified by the thickness in percent of the chord length. These comparisons were made at a speed of 30 fps which was sufficiently high to avoid Froude effects; this was the highest speed

at which there were no apparent cavitation effects for any of the models. For the thin flat plate (ref. 2), at 30 fps, the only data available were at angles of attack from 0° to 8°.

The plot of lift coefficient against geometric angle of attack in figure 6 shows that the cambered models had lower angles of zero lift, lower lift-curve slopes, and lower lift coefficients at the high angles of attack than the flat-plate models. It may be noted in this figure that for the cambered models the lift coefficient increased with increasing thickness while the lift coefficients for the flat-plate models decreased with increasing thickness. These facts are true for the geometric angle of attack since the angles of zero lift for the flat-plate models are 0° and for the cambered models are at some lower angle of attack with the thickest model having the lowest angle of zero lift. However, when the lift coefficient is plotted against the angle of attack measured from the angle of zero lift (also shown in fig. 6), the lift coefficient decreased with increasing thickness for the cambered models as well as for the flat-plate models. It can be seen in this figure that the lift-curve slope decreased with increasing thickness. The nonlinearity of the lift curve, found in all low-aspect-ratio results, is evident for all models.

The lift-drag polar (fig. 7) shows that the drag coefficient at any given lift coefficient increased with increasing thickness. The plot of lift-drag ratio against lift coefficient in figure 7 shows that for a given lift coefficient the lift-drag ratio decreased with increasing thickness. The range of maximum lift-drag ratio from 3.5 to 5 occurred over a range of lift coefficients from 0.125 for the thin flat plate at an angle of attack of 8° to 0.175 for the thick cambered model at an angle of attack of 13°. Therefore, the maximum lift-drag ratio moved to higher angles of attack with increasing thickness.

The effect of increasing camber, which also increased the thickness, on the lift coefficient is shown in figure 8 where the lift coefficient is plotted against thickness in percent of chord. Figure 8 shows that for the range of thicknesses investigated the lift coefficient changed as a linear function of thickness with this change diminishing as the angle of attack was increased. At an angle of attack of 20° the lift coefficient remained about constant with increase in thickness ratio.

The location of the center of pressure as a function of angle of attack is shown in figure 9 for the flat-plate models and the cambered models. The centers of pressure moved rearward with decreasing angle of attack for the cambered models. This is in contrast with the centers of pressure for the flat-plate models which moved forward with decreasing angle of attack. For any given angle of attack the center-of-pressure locations for the cambered models were always aft of those for the flat-plate models.

CONCLUSIONS

The results of the investigation indicated the following conclusions:

1. The addition of camber, which increased the thickness, decreased the angle of zero lift, the lift-curve slope, and the lift coefficients at the high angles of attack.

2. For a given lift coefficient, the maximum lift-drag ratio decreased with increasing camber. The maximum lift-drag ratio moved to higher angles of attack with increasing camber.

3. As the camber on the upper surface was increased, thus increasing the thickness from approximately 7 to 10 percent chord and for a given angle of attack, the lift coefficient changed as a linear function of thickness.

4. The center of pressure of the cambered surfaces moved rearward with decreasing angle of attack while the center of pressure of the flat plates moved forward with decreasing angle of attack.

Langley Research Center,
National Aeronautics and Space Administration,
Langley Field, Va., August 19, 1959.

REFERENCES

1. Vaughan, Victor L., Jr., and Ramsen, John A.: Hydrodynamic Characteristics Over a Range of Speeds up to 80 Feet Per Second of a Rectangular Modified Flat Plate Having an Aspect Ratio of 0.25 and Operating at Several Depths of Submersion. NACA TN 3908, 1957.

2. Wadlin, Kenneth L., Ramsen, John A., and Vaughan, Victor L., Jr.: The Hydrodynamic Characteristics of Modified Rectangular Flat Plates Having Aspect Ratios of 1.00, 0.25, and 0.125 and Operating Near a Free Water Surface. NACA Rep. 1246, 1955.

3. Ramsen, John A., and Vaughan, Victor L., Jr.: Hydrodynamic Tares and Interference Effects for a 12-Percent-Thick Surface-Piercing Strut and an Aspect-Ratio-0.25 Lifting Surface. NACA TN 3420, 1955.

4. Ramsen, John A.: An Experimental Hydrodynamic Investigation of the Inception of Vortex Ventilation. NACA TN 3903, 1957.

TABLE I

COORDINATES OF UPPER SURFACE OF THICK CAMBERED MODEL

[Thickness, 9.88 percent chord]

x, in.	y, in.
0.046	0.1485
.078	.184
.145	.239
.315	.343
.665	.494
1.016	.612
1.396	.709
2.080	.867
2.790	.988
3.520	1.080
4.217	1.146
4.932	1.190
5.644	1.209
6.358	1.201
7.070	1.168
7.780	1.117
8.480	1.046
9.180	.962
9.885	.862
10.580	.746
11.290	.617
12.000	.469
12.710	.317
13.420	.159
14.140	.0035

TABLE II

COORDINATES OF UPPER SURFACE OF MEDIUM CAMBERED MODEL

[Thickness, 8.60 percent chord]

x, in.	y, in.
0.058	0.143
.092	.174
.161	.223
.334	.315
.686	.445
1.038	.544
1.392	.627
2.100	.758
2.808	.857
3.518	.931
4.228	.984
4.938	1.017
5.648	1.028
6.359	1.015
7.069	.981
7.779	.929
8.489	.863
9.198	.784
9.907	.693
10.616	.593
11.325	.485
12.031	.368
12.735	.248
13.438	.126
14.140	.0035

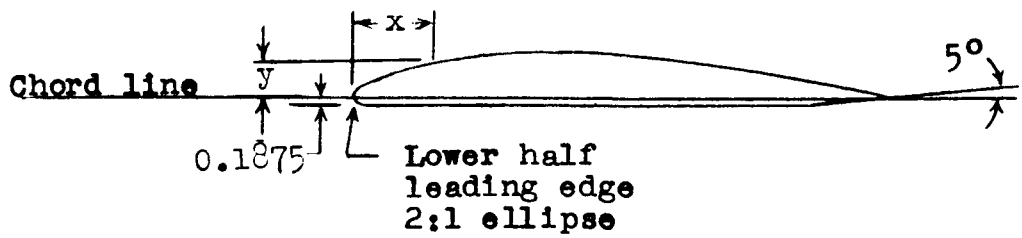

TABLE III

COORDINATES OF UPPER SURFACE OF

THIN CAMBERED MODEL

[Thickness, 7.02 percent chord]

x, in.	y, in.
0.046	0.099
.078	.123
.145	.159
.315	.228
.665	.329
1.016	.408
1.396	.472
2.080	.577
2.790	.658
3.520	.719
4.217	.763
4.932	.793
5.644	.805
6.358	.799
7.070	.778
7.780	.744
8.480	.697
9.180	.641
9.885	.574
10.580	.497
11.290	.411
12.000	.312
12.710	.211
13.420	.106
14.140	.0023

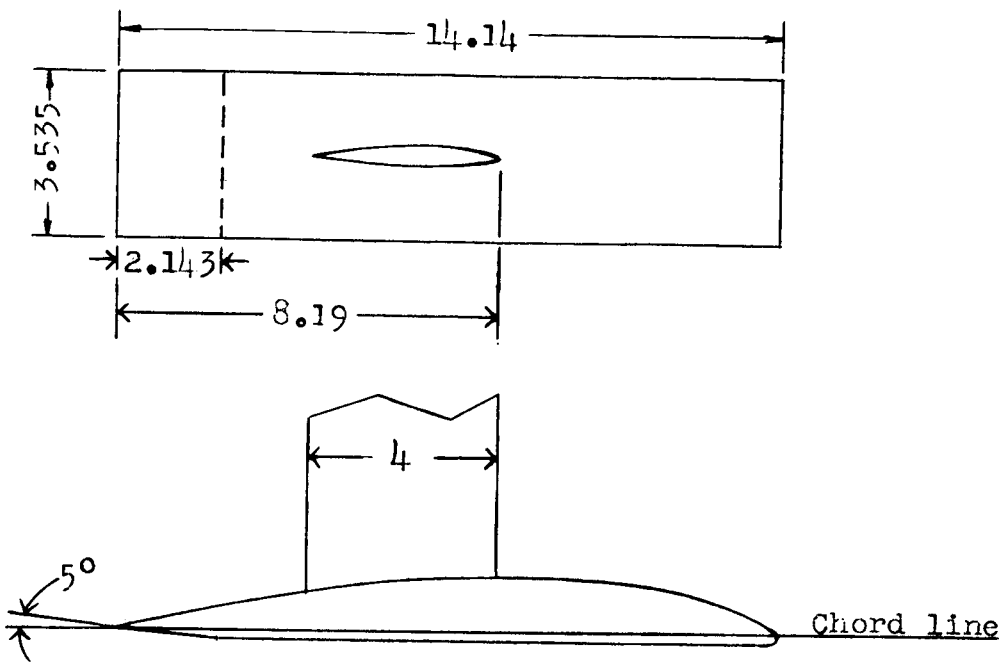

Thick cambered model
(thickness, 9.88 percent chord)

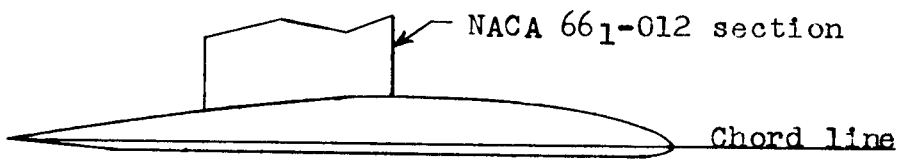

Medium cambered model
(thickness, 8.60 percent chord)

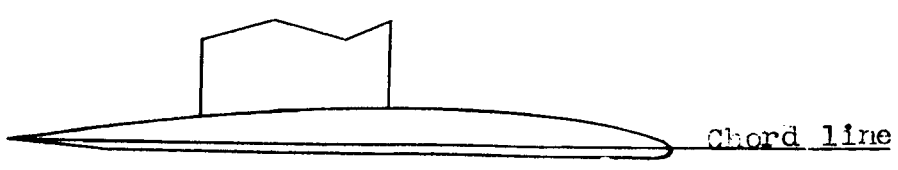

Thin cambered model
(thickness, 7.02 percent chord)

Figure 1.- Details of models. (Dimensions are in inches.)

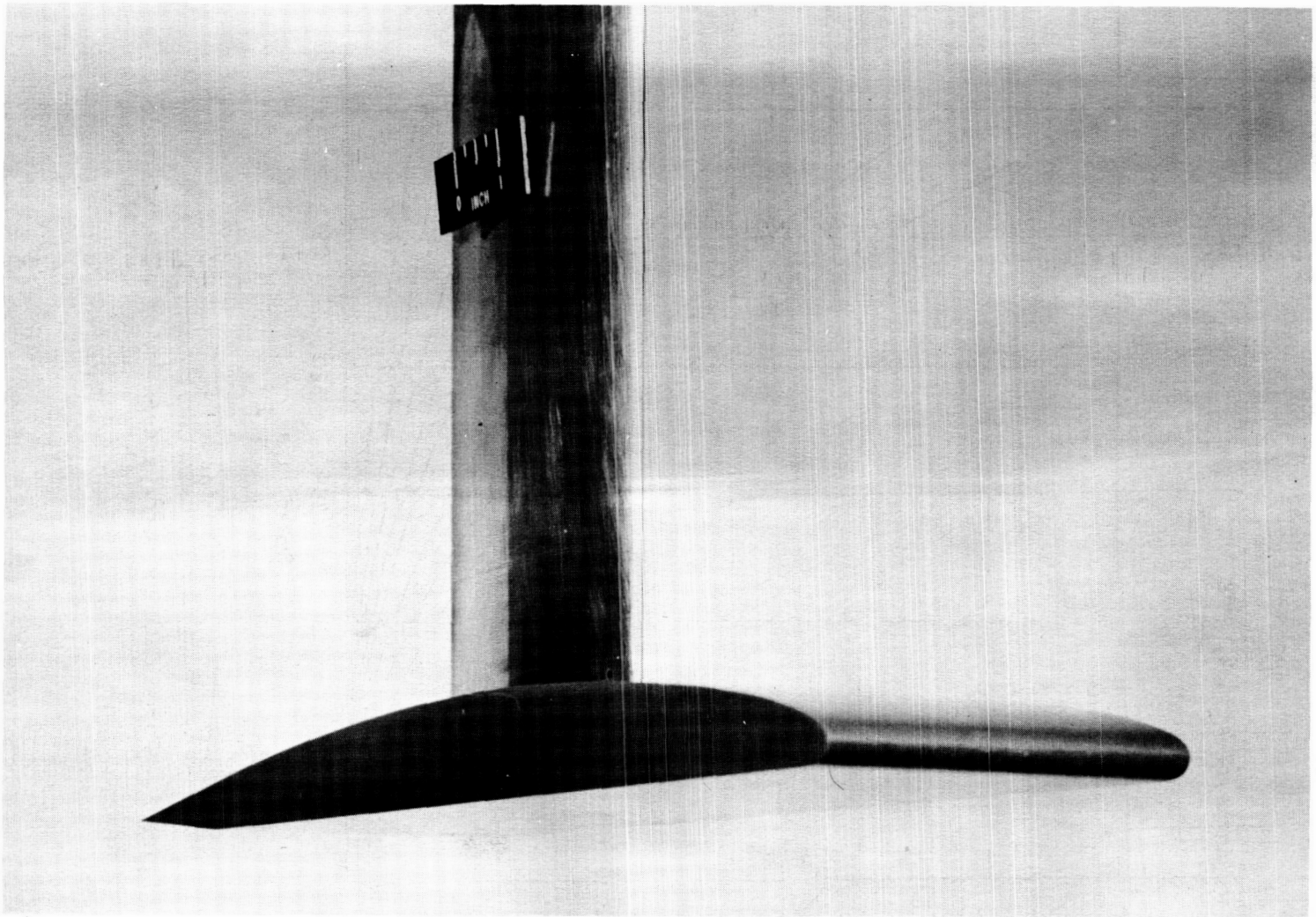

Figure 2.- Photograph of typical model. L-95334

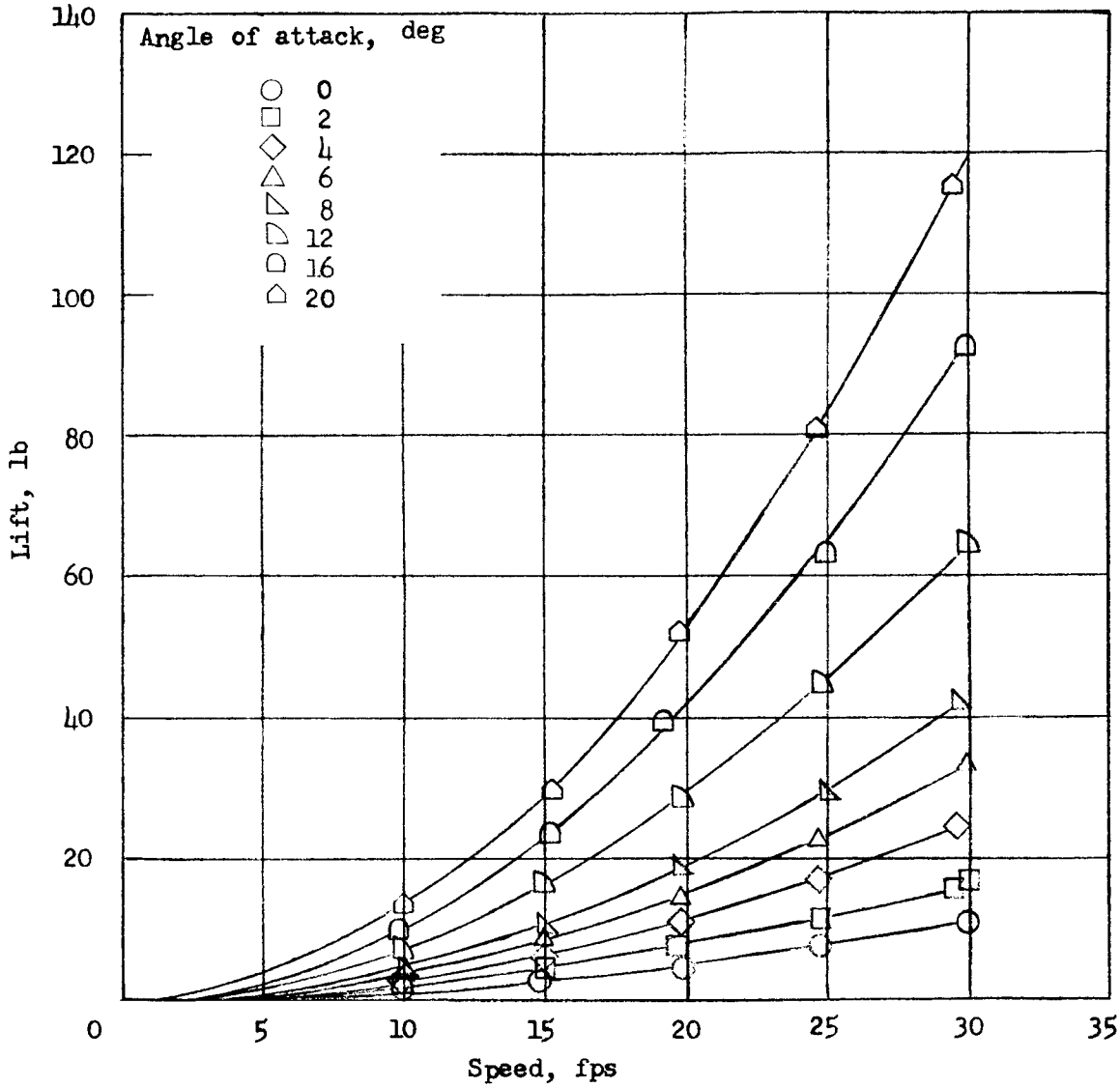

(a) Lift.

Figure 3.- Force data on 9.88-percent-thick cambered model.

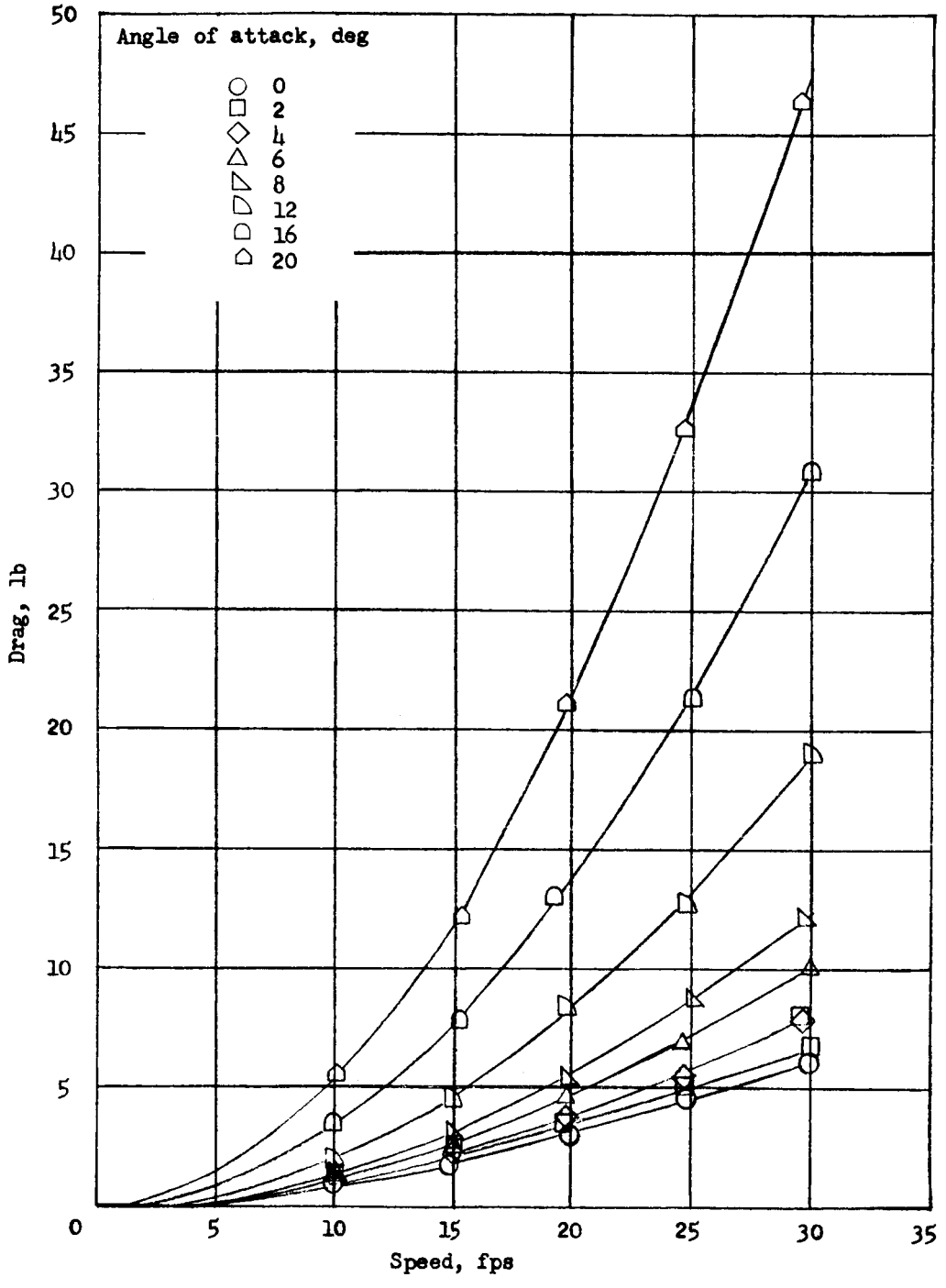

(b) Drag.

Figure 3.- Continued.

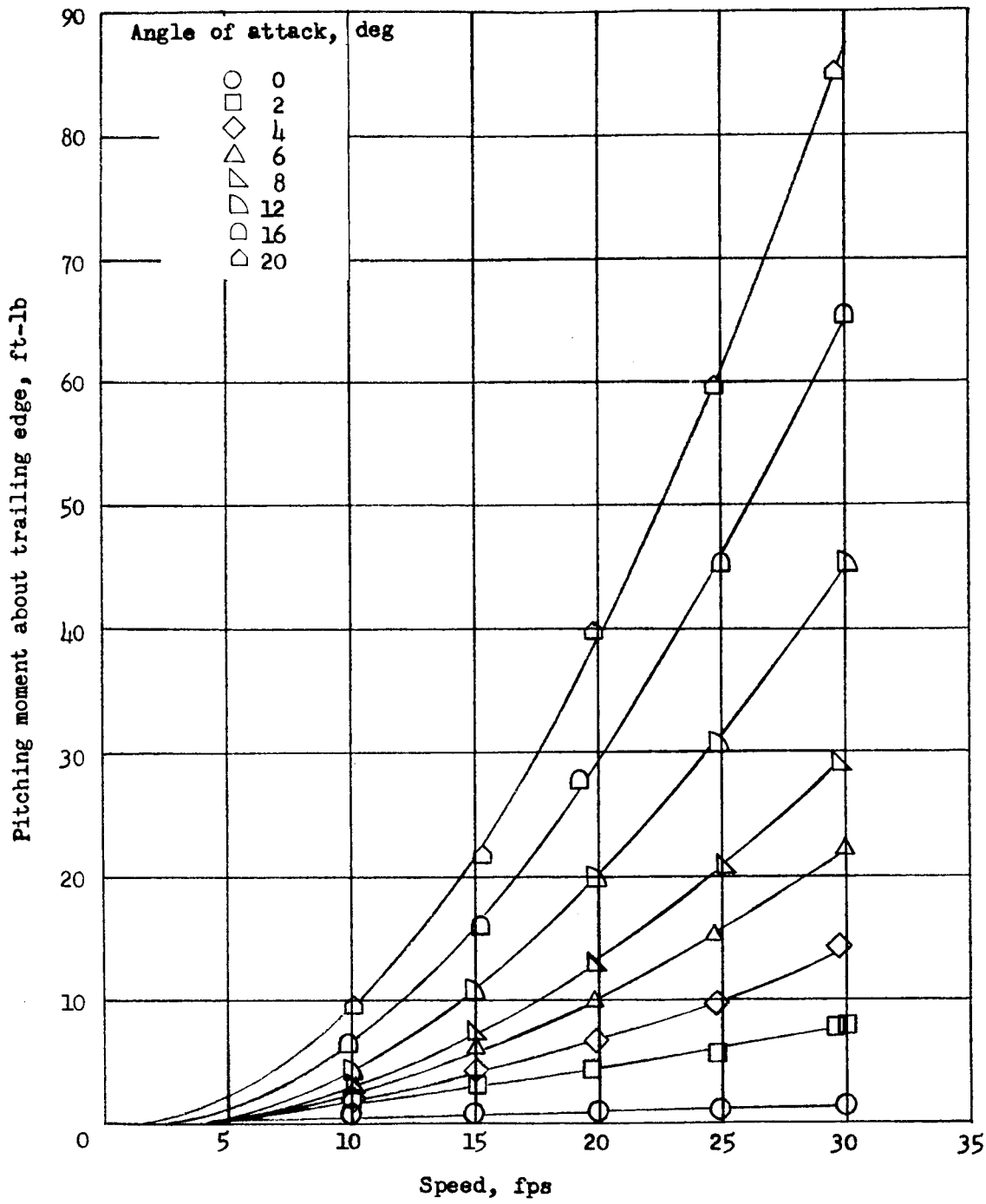

(c) Pitching moment.

Figure 3.- Concluded.

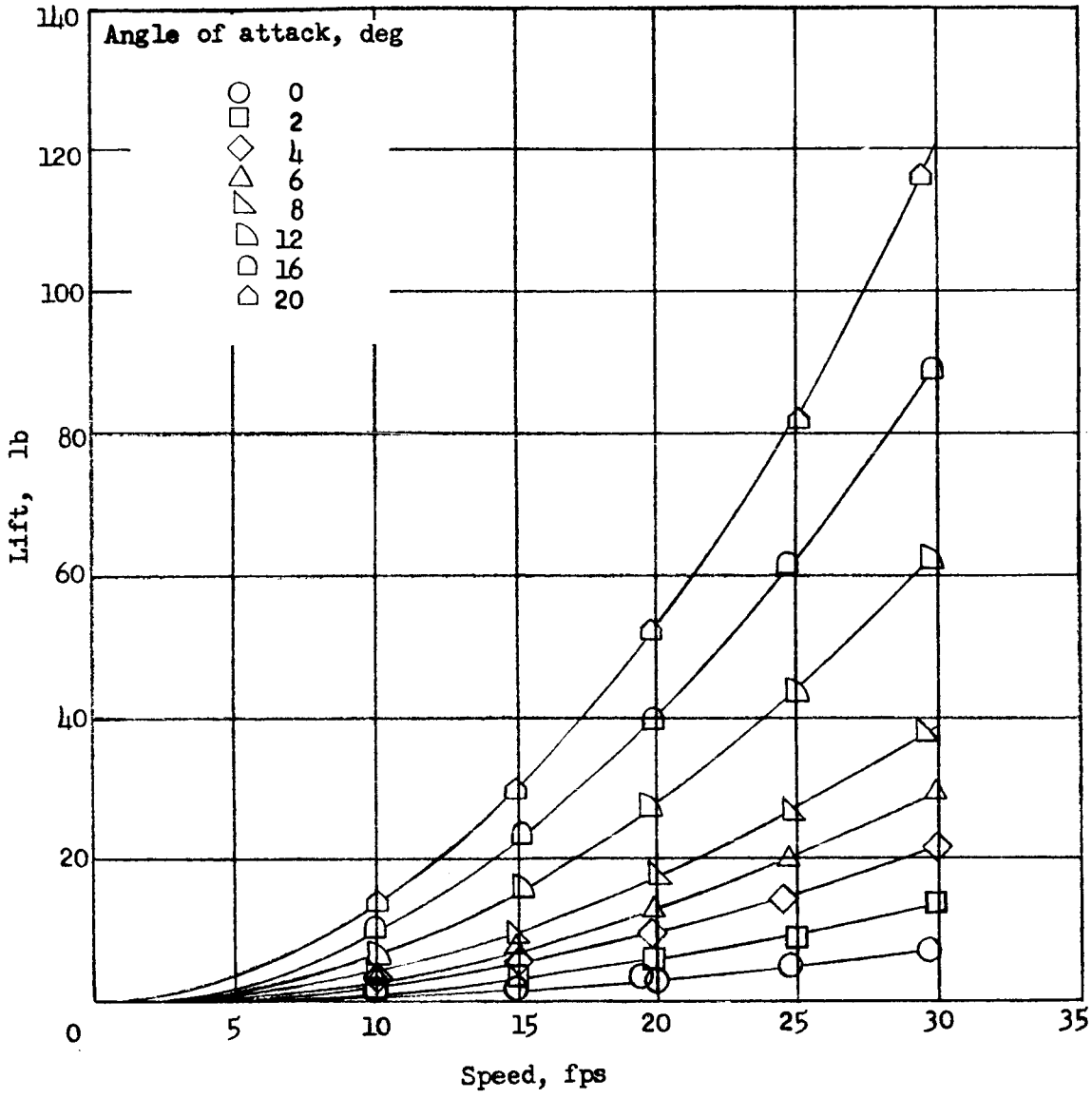

(a) Lift.

Figure 4.- Force data on 8.60-percent-thick cambered model.

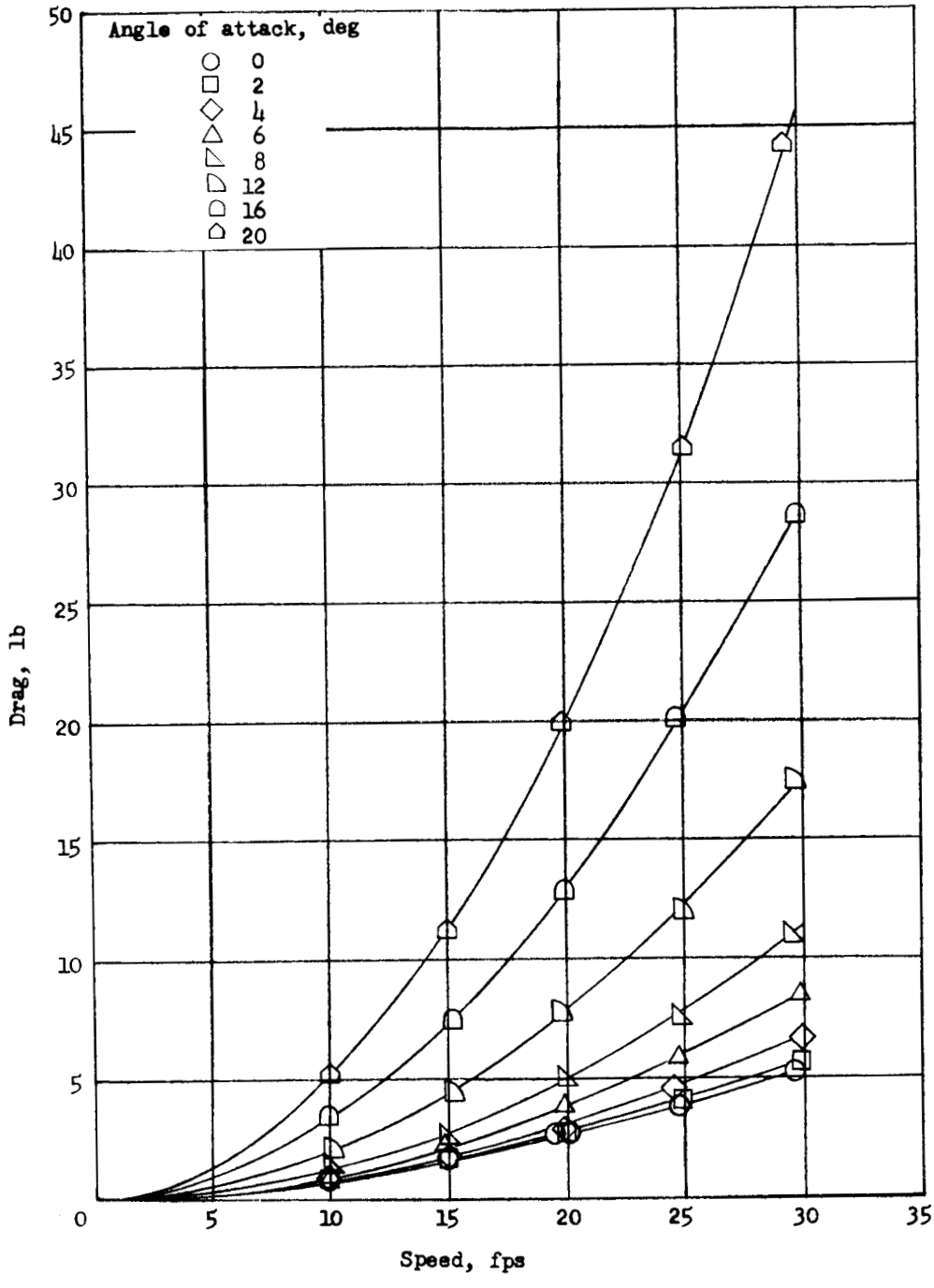

(b) Drag.

Figure 4.- Continued.

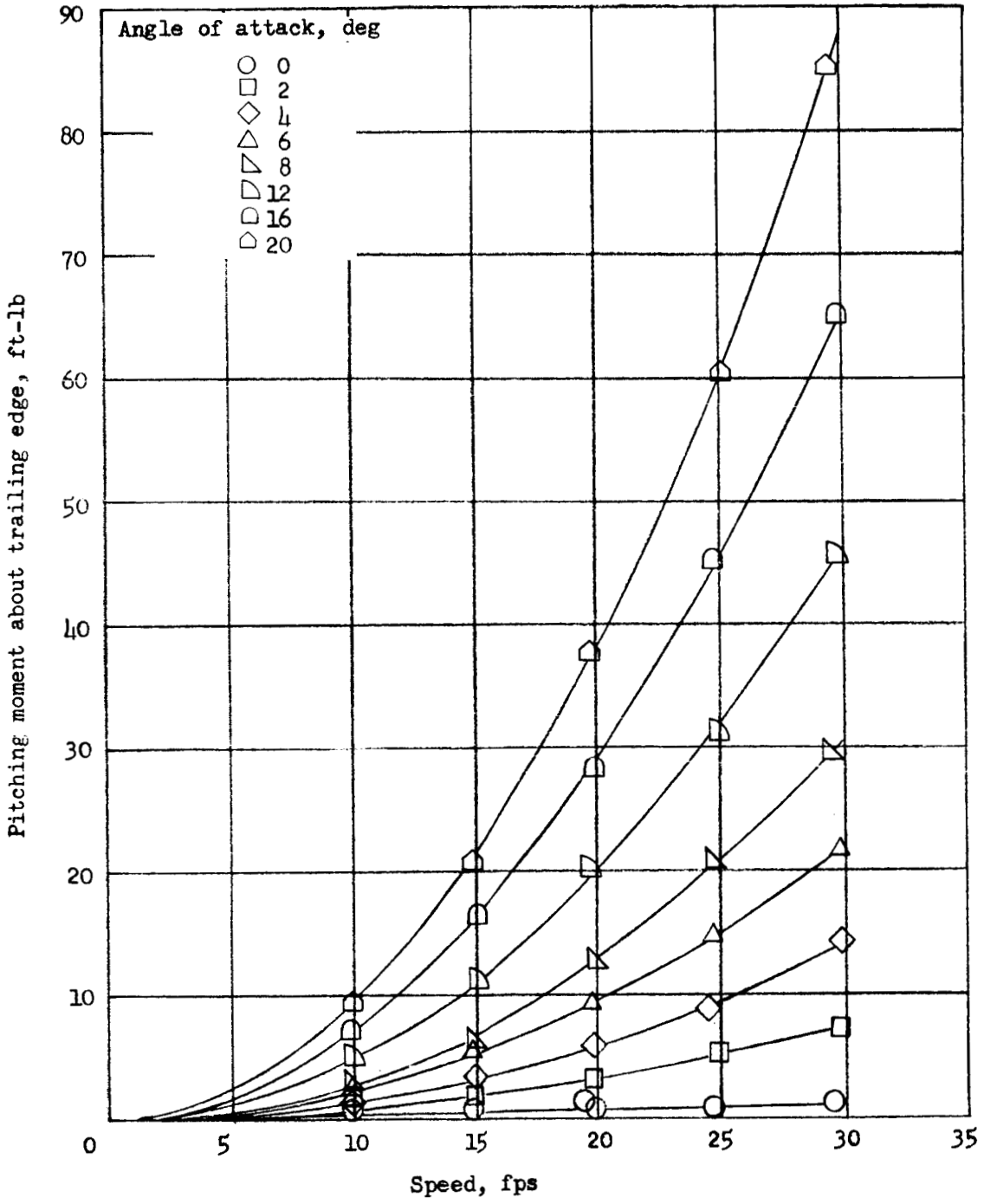

(c) Pitching moment.

Figure 4.- Concluded.

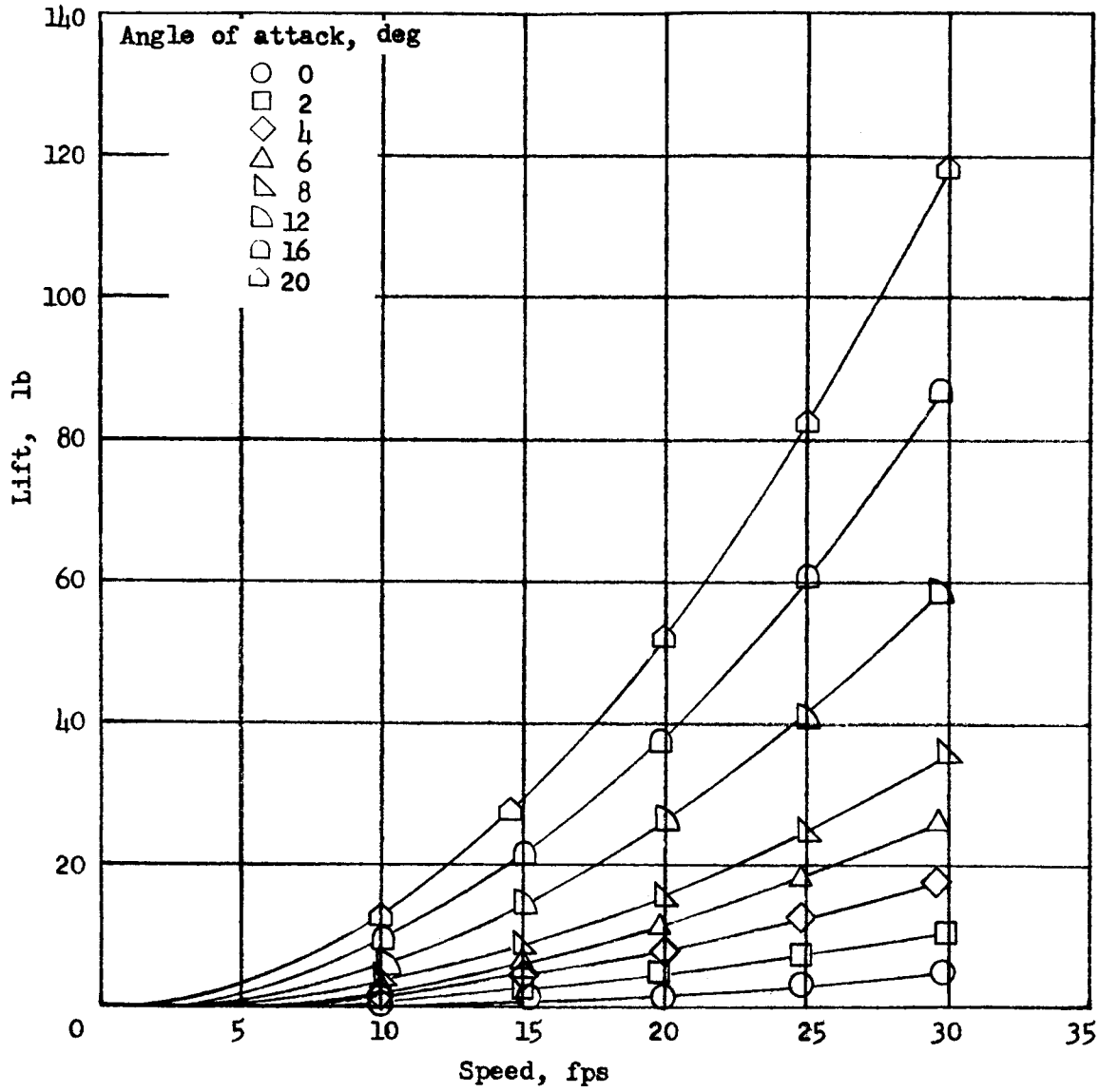

(a) Lift.

Figure 5.- Force data on 7.02-percent-thick cambered model.

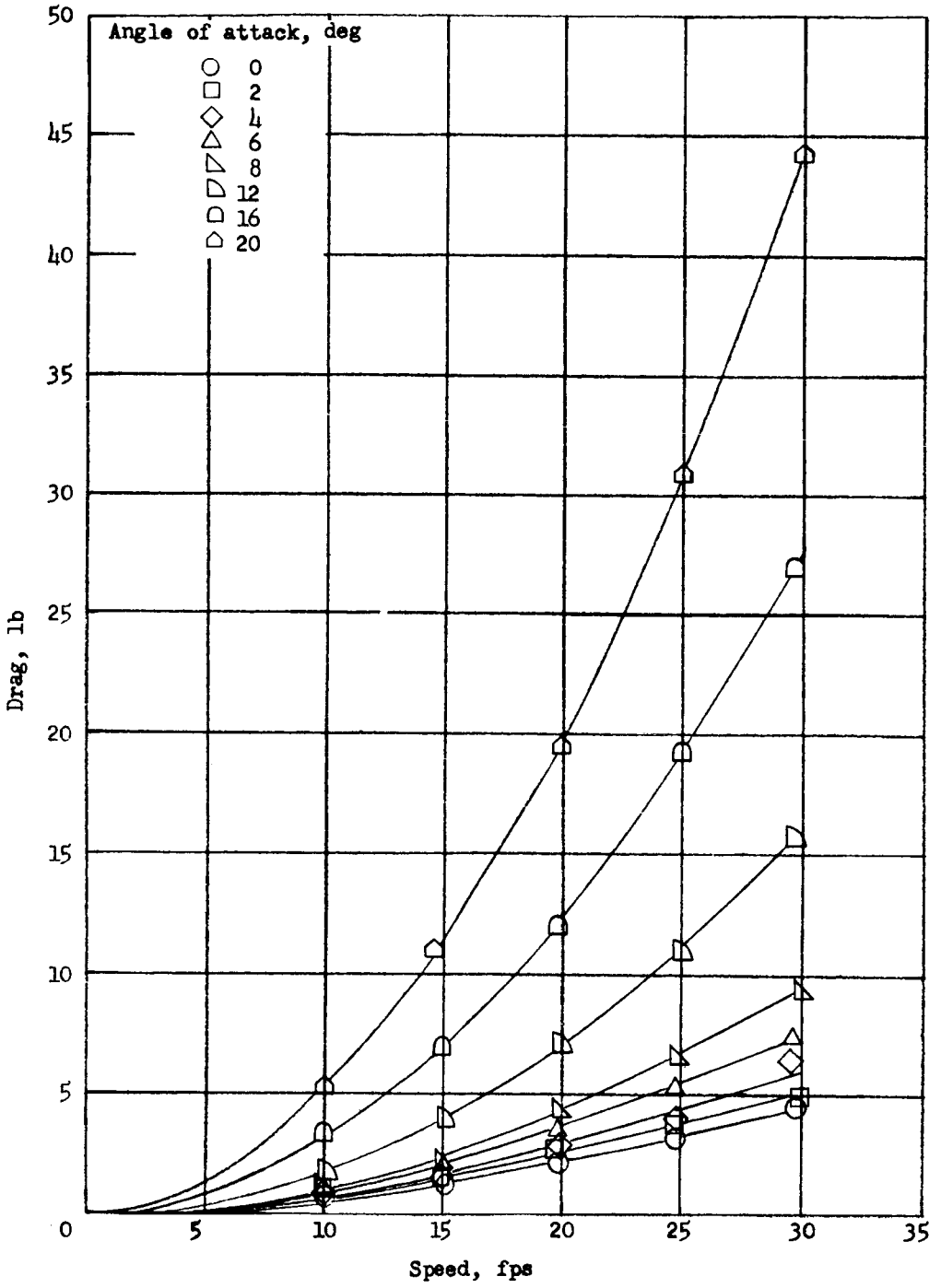

(b) Drag.

Figure 5.- Continued.

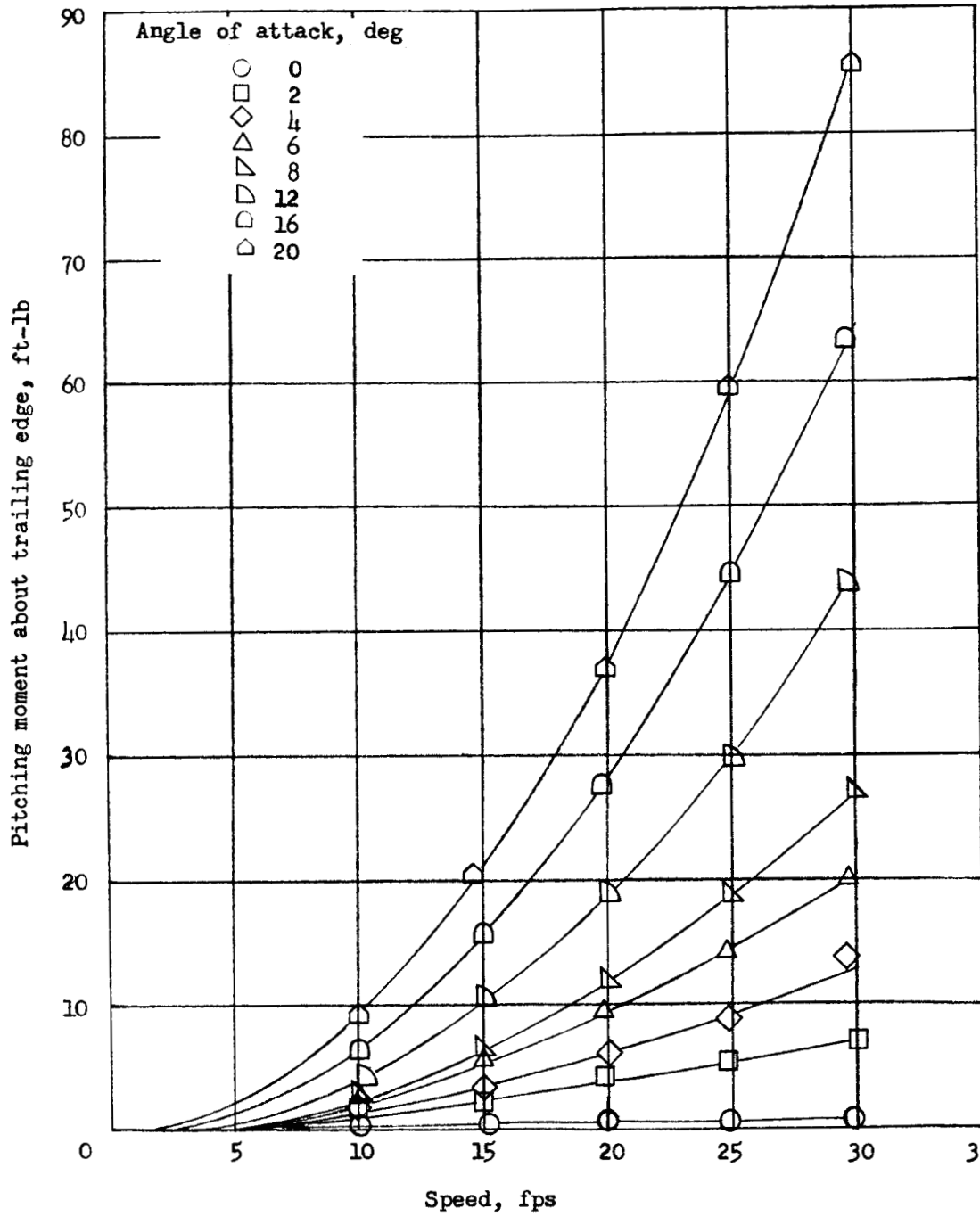

(c) Pitching moment.

Figure 5.- Concluded.

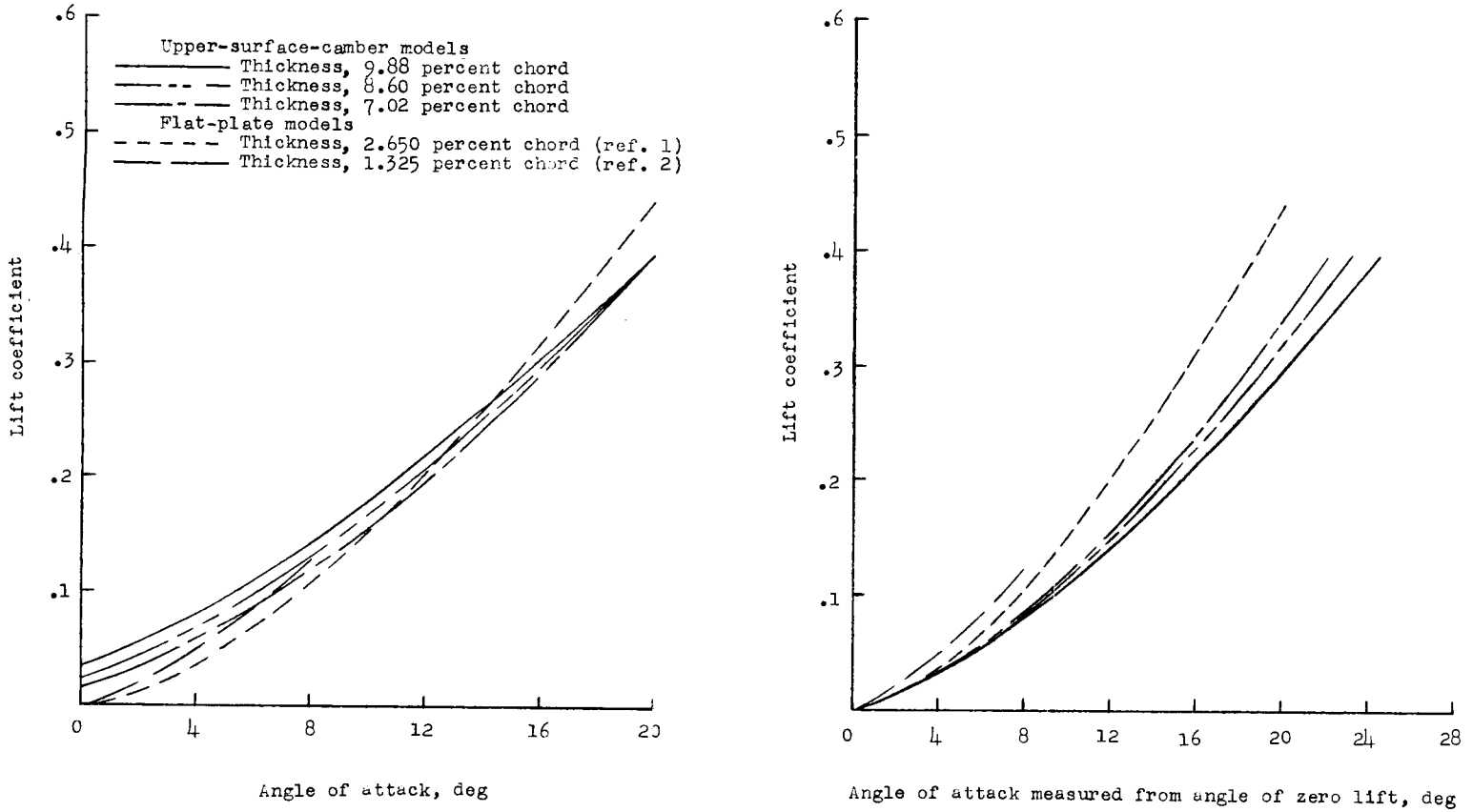

Figure 6.- Comparison of lift characteristics at a speed of 30 fps.

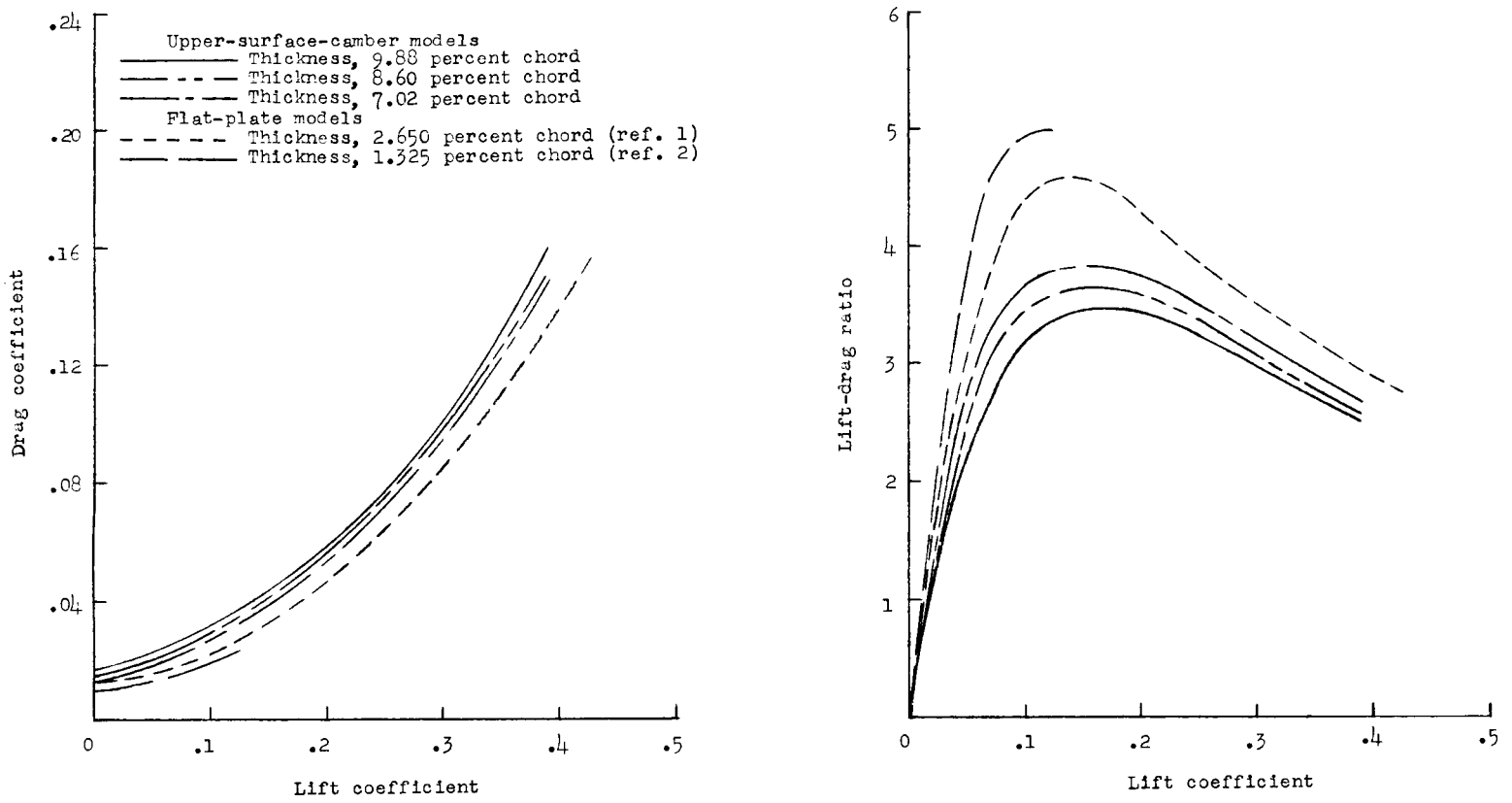

Figure 7.- Comparison of drag characteristics and of lift-drag ratios at a speed of 30 fps.

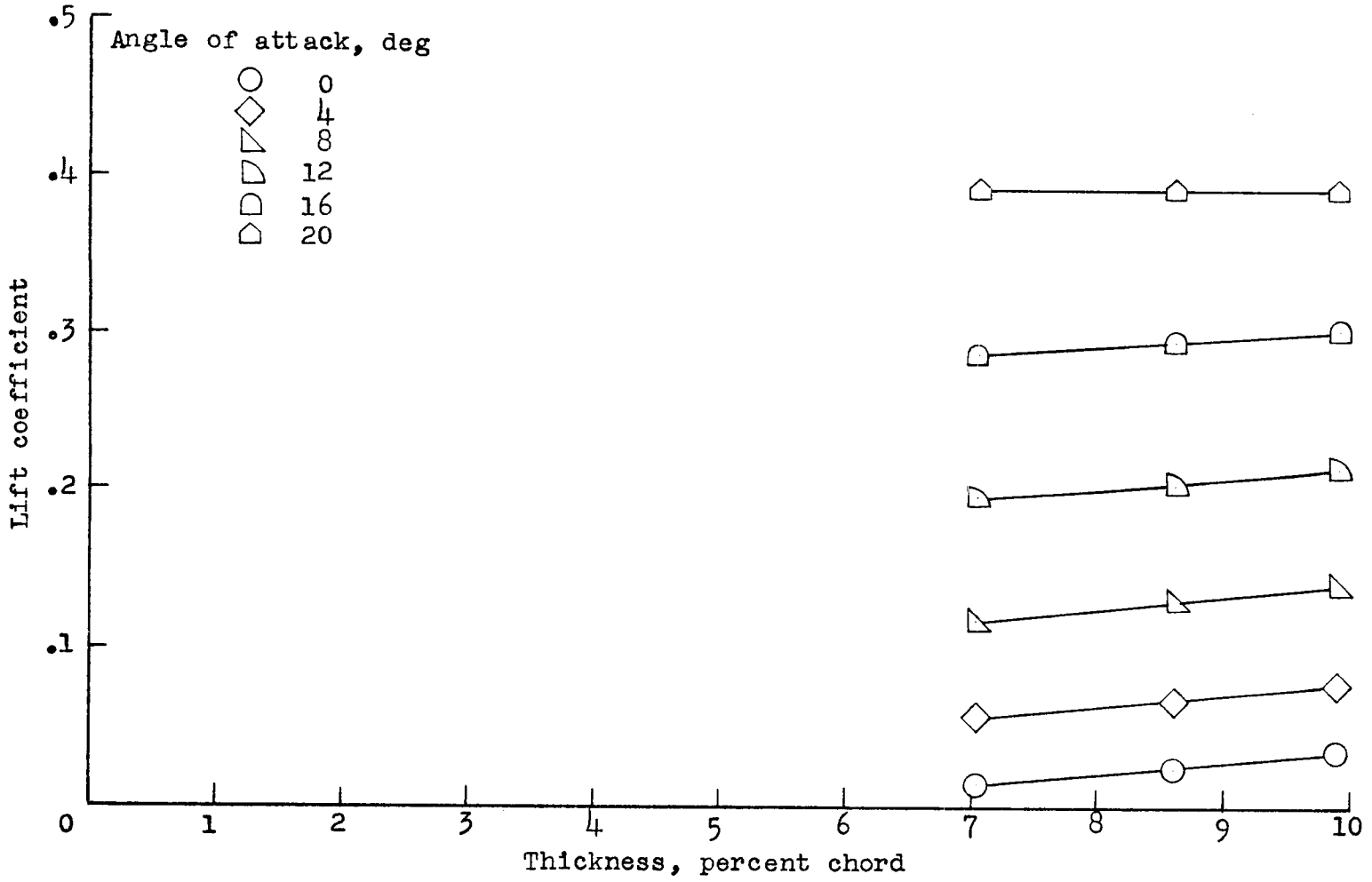

Figure 8.- Effect of thickness ratio on cambered models at a speed of 30 fps.

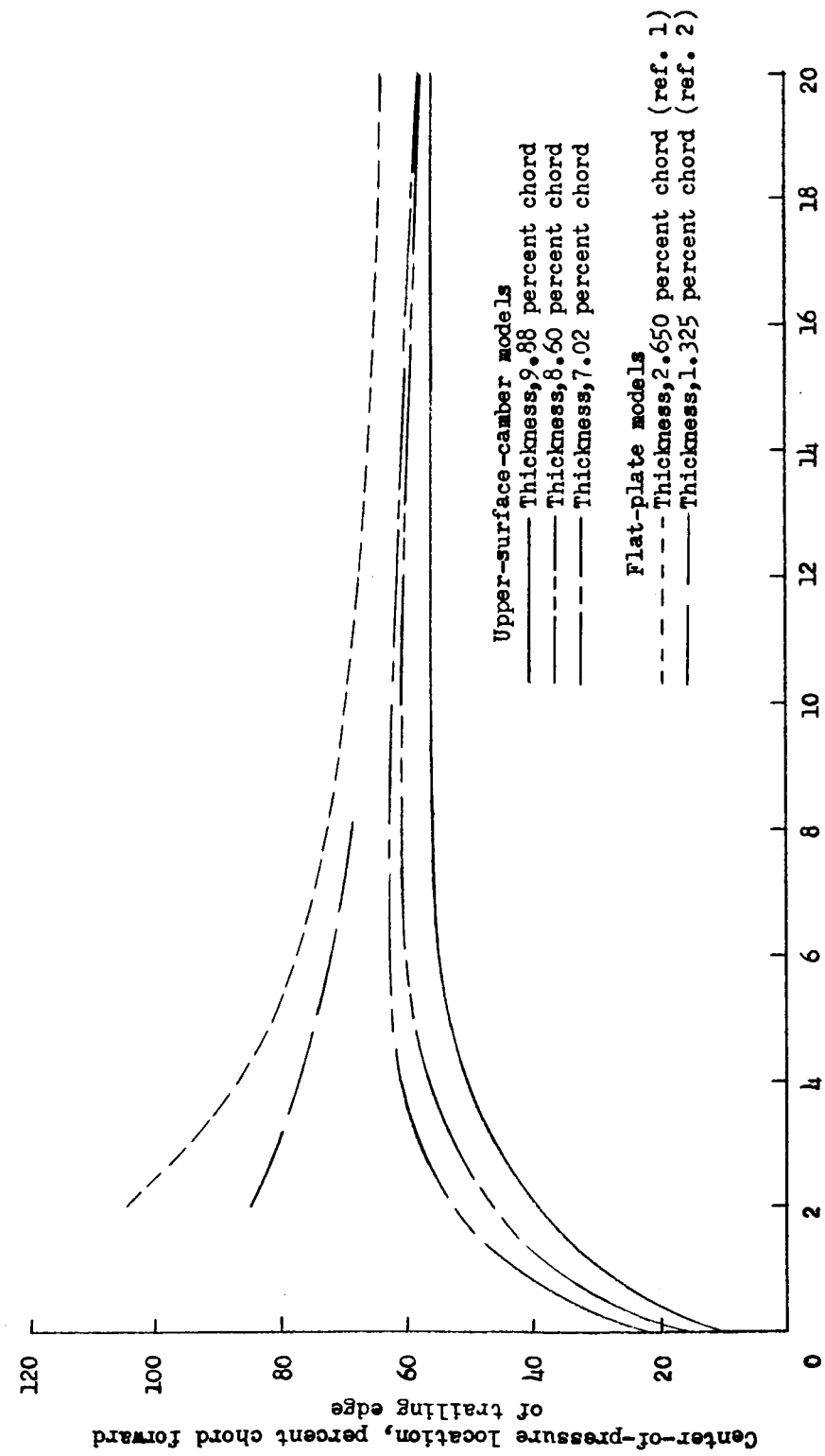

Figure 9.- Comparison of center-of-pressure locations for upper-surface-camber models and flat-plate models at a speed of 30 fps.